International Communications in Heat and Mass Transfer 36 (2009) 921–924

Contents lists available at ScienceDirect

International Communications in Heat and Mass Transfer

journal homepage: www.elsevier.com/locate/ichmt

# An investigation of a mixed convection in a ⊔ shape channel moving with a reciprocating motion☆

Wu-Shung Fu *, Sin-Hong Lian, Yu-Chih Lai

*Department of Mechanical Engineering, National Chiao Tung University, 1001 Ta Hsueh Road, Hsinchu, 30056, Taiwan, ROC*

ARTICLE INFO

Available online 1 July 2009

*Keywords:*
Mixed convection
Moving boundary
ALE
Reciprocating motion

ABSTRACT

This study focuses on utilizing numerical calculation to investigate the heat transfer mechanisms in a ⊔ shape reciprocating channel system comprised of a horizontal channel at the bottom and vertical channels on both left and right sides. The issue is considered one kind of moving boundary problems and the finite element and Arbitrary Lagrangian–Eulerian (ALE) kinematic methods can be applied to this study. Due to the high temperature at the bottom surface of the horizontal channel and the direction of inlet cooling fluids in the same direction of the gravity, the heat transfer mechanisms induced by the mixed convection flow become extremely complex. The results show that thermal layers near the heat surface are disturbed drastically and the effect of reciprocating motion upon the heat transfer mechanisms strongly depends on a relationship between Reynolds and Grashof numbers.



## 1. Introduction

Protecting a piston from heat damage could effectively enhance the thermal efficiency of the heat engine and economize the usage of energy [1]. Numerous studies were then to investigate similar objects. In order to simulate the heat transfer phenomena of pistons in a reciprocating motion more realistically, the heat dissipation phenomena in a ⊔ shape reciprocating channel assumed as the piston action have been studied numerically by the authors and the related studies were reviewed in detail in [2].

In the previous study [2] the forced convection mechanisms were investigated exclusively. However, the temperature of pistons is usually very high and the effect of natural convection on the heat transfer mechanisms of the reciprocating object needs to be considered also. Thus this study aims to investigate the numerical calculation of the mixed convection mechanisms in the ⊔ shape reciprocating channel. Effects of Reynolds and Grashof numbers on the heat transfer mechanisms are examined in detail.

Usually when the problem of mixed convection is investigated, the relationship between the directions of inlet cooling fluids and gravity, and the positions of heat region relative to the direction of gravity should be examined first. In this study the vertical channels on the left and right sides provide the cooling fluids to flow into and out of the ⊔ shape channel, respectively. A heat region is installed at the bottom of the horizontal channel in the ⊔ shape channel system. The inlet cooling fluids have the same direction as the gravity. Due to the position of heat region, the phenomena of opposite and aiding flows can be observed in the left and right channels, respectively. Additionally, because of the mutual counteractions caused by the buoyancy of upward direction and the impulse of cooling fluids in a horizontal direction, thermal layers attaching to the heat region of horizontal channel will be disturbed drastically. As a result, the local Nusselt numbers distributed on the heat surface vary with time in a periodical duration. These interesting and complicated phenomena have not been investigated yet.

## 2. Physical model

A physical model implemented in this study is shown in Fig. 1. The total channel width and length are $w_0$ and $h_0$, respectively, and the channel width is $w$. The horizontal channel means the region surrounded by $\overline{BO'FGP'C}$. The bottom surface $\overline{BC}$ is heat surface and at constant temperature $T_{H.}$ Besides, the temperature and velocity of inlet cooling fluids are $T_0$ and $v_0$, respectively. Other surfaces of the channel are insulated. The original length between $\overline{OP}$ and $\overline{MN}$ is $w$ and the maximum elongation length is $2w$. A part of the channel circled by $\overline{M'BCN'G'GFF'}$ is called as a reciprocating channel. The adjustable length $w$ is the moving distance of the reciprocating channel. Therefore, computational grids in this region are flexible. As the channel moves downward, $\overline{MN}$ is fixed and $\overline{OP}$ moves downward with a velocity of $v_c$, the original region is then elongated. Afterward the $\overline{OP}$ moves upward and returns to the original position. The mesh velocity of the computational grids inside the horizontal channel is equal to that of $\overline{OP}$. The right channel length $h_l$ is long enough for satisfying the convergent conditions of the temperature and velocity at the outlet of the channel. The reciprocating velocity of the horizontal channel is $v_c$,

☆ Communicated by W.J. Minkowycz.

* Corresponding author.
*E-mail addresses:* wsfu@mail.nctu.edu.tw (W.-S. Fu), edenas.me94g@nctu.edu.tw (S.-H. Lian).

0735-1933/$ – see front matter © 2009 Elsevier Ltd. All rights reserved.
doi:10.1016/j.icheatmasstransfer.2009.06.006

**Nomenclature**

| | |
|---|---|
| $F_c$ | dimensionless reciprocating frequency of the piston |
| $Gr$ | Grashof number |
| $h_1$ | dimensional height of the inlet channel and outlet channel [m] |
| $L_c$ | dimensionless reciprocating amplitude of the piston |
| $Nu_X$ | local Nusselt number |
| $\overline{Nu}_X$ | average Nusselt number on the heat surface |
| $\overline{Nu}_c$ | time-average Nusselt number per cycle |
| $p$ | dimensional pressure [N m$^{-2}$] |
| $p_\infty$ | reference pressure [N m$^{-2}$] |
| $P$ | dimensionless pressure |
| $Pr$ | Prandtl number |
| $Re$ | Reynolds number |
| $t$ | dimensional time [s] |
| $T$ | dimensional temperature [K] |
| $u$, $v$ | dimensional velocities of in $x$ and $y$ directions [m s$^{-1}$] |
| $v_0$ | dimensional velocities of the inlet fluid [m s$^{-1}$] |
| $U$, $V$ | dimensionless velocities of in $X$ and $Y$ directions |
| $V_c$ | dimensionless reciprocating velocity of the piston |
| $V_m$ | dimensionless maximum reciprocating velocity of the piston |
| $\hat{V}$ | dimensionless mesh velocity in $y$-direction |
| $x$, $y$ | dimensional Cartesian coordinates [m] |
| $X$, $Y$ | dimensionless Cartesian coordinates |

*Greek symbols*

| | |
|---|---|
| $\alpha$ | thermal diffusivity [m$^2$ s$^{-1}$] |
| $\nu$ | kinematics viscosity [m$^2$ s$^{-1}$] |
| $\eta_0$ | total length of the moving mesh region |
| $\eta_1$ | length counted from the bottom of the moving mesh region |
| $\theta$ | dimensionless temperature |
| $\rho$ | density [kg m$^{-3}$] |
| $\tau$ | dimensionless time |

and can be expressed as the equation, $v_c = v_m \sin(2\pi f_c t)$, where $v_m$ is the maximum reciprocating velocity of the piston and equals to $2\pi f_c l_c$. When the channel moves reciprocally, it will cause the motions of the cooling fluids to be time-dependent. The circumstance is regarded as a moving boundary problem and therefore the Arbitrary Lagrangian–Eulerian (ALE) method is properly applied to this study.

For facilitating the analysis, the following assumptions are made.

(1) The fluid is air and the flow field is two-dimensional, incompressible and laminar.
(2) Except the density of the fluid, other properties of the fluid are assumed to be constant, and Boussinesq assumption is adopted.
(3) Apply the no-slip condition to all boundaries. Thus the fluid velocity on the moving boundaries is equal to the moving velocity of the boundaries.

Based upon the characteristics scales of $w$, $v_0$, $\rho v_0^2$, and $T_0$, the dimensionless variables are defined as follows:

$$X = \frac{x}{w}, \quad Y = \frac{y}{w}, \quad U = \frac{u}{v_0}, \quad V = \frac{v}{v_0}, \quad \hat{V} = \frac{\hat{v}}{v_0}, \quad V_m = \frac{v_m}{v_0}, \quad V_c = \frac{v_c}{v_0}$$
$$F_c = \frac{f_c w}{v_0}, \quad P = \frac{p - p_\infty}{\rho v_0^2}, \quad \tau = \frac{t v_0}{w}, \quad \theta = \frac{T - T_0}{T_h - T_0}, \quad Re = \frac{v_0 w}{\nu}, \quad Pr = \frac{\nu}{\alpha}$$
$$Gr = \frac{g\beta(T_h - T_0)w^3}{\nu^2}, \quad V_c = V_m \sin(2\pi F_c \tau) \tag{1}$$

and $\hat{v}$ is defined as the mesh velocity.

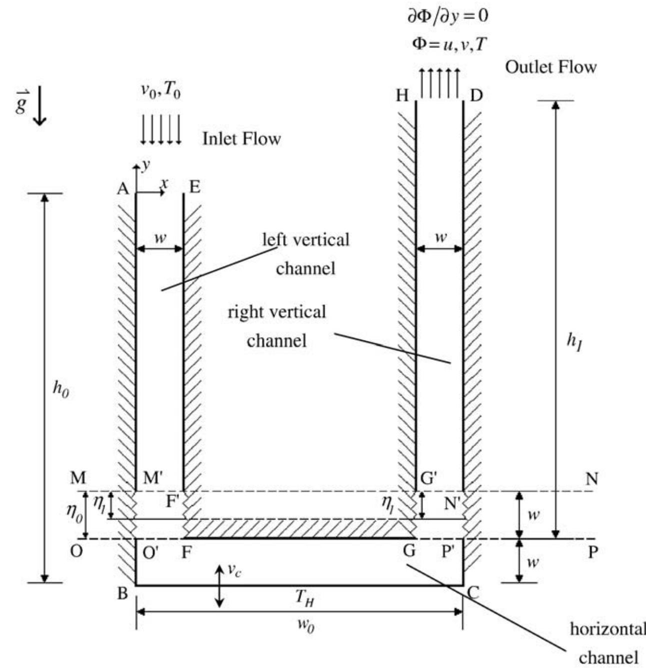


**Fig. 1.** Physical model of the ⊔ shape channel.

According to the above assumptions and dimensionless variables, the dimensionless ALE governing equations are expressed as the following equations:

*Continuity equation*

$$\frac{\partial U}{\partial X} + \frac{\partial V}{\partial Y} = 0 \tag{2}$$

*Momentum equation*

$$\frac{\partial U}{\partial \tau} + U\frac{\partial U}{\partial X} + \left(V - \hat{V}\right)\frac{\partial U}{\partial Y} = -\frac{\partial P}{\partial X} + \frac{1}{Re}\left(\frac{\partial^2 U}{\partial X^2} + \frac{\partial^2 U}{\partial Y^2}\right) \tag{3}$$

$$\frac{\partial V}{\partial \tau} + U\frac{\partial V}{\partial X} + \left(V - \hat{V}\right)\frac{\partial V}{\partial Y} = -\frac{\partial P}{\partial Y} + \frac{1}{Re}\left(\frac{\partial^2 V}{\partial X^2} + \frac{\partial^2 V}{\partial Y^2}\right) + \frac{Gr}{Re^2}\theta \tag{4}$$

*Energy equation*

$$\frac{\partial \theta}{\partial \tau} + U\frac{\partial \theta}{\partial X} + \left(V - \hat{V}\right)\frac{\partial \theta}{\partial Y} = \frac{1}{Re\,Pr}\left(\frac{\partial^2 \theta}{\partial X^2} + \frac{\partial^2 \theta}{\partial Y^2}\right) \tag{5}$$

In this study, the cooling channel moves only in a vertical direction and therefore the horizontal mesh velocity is absent in the above governing equations. According to ALE method, the mesh velocity $\hat{V}$ is linearly distributed in the region between $\overline{MN}$ (fixed) and $\overline{OP}$ (movable). The mesh velocity $V_{\eta 1}$ at the position $\eta_1$ is proportional to the distance between $\overline{MN}$ and $\overline{OP}$, and is defined as the following equation,

$$V_{\eta_1} = \frac{\eta_1}{\eta_0} \cdot V_c \tag{6}$$

In the other regions, the mesh velocities are all set to be 0. The boundary conditions and solutions method used in this study are similar to those adopted in [2] except the term $Gr/Re^2$ taken into consideration in Eq. (4).

## 3. Results and discussion

The working fluid is air ($Pr = 0.7$). Combinations of main parameter are tabulated in Table 1. To obtain the optimal computational mesh, three models with different number of elements are used for mesh tests. According to the results, the computational mesh with 20,020 elements which correspond to 61,983 nodes is used through all analysis in this study. The local Nusselt number $Nu_X$ of the heat surface at time $\tau$, the average Nusselt number $\overline{Nu}_X$ of the heat surface at time $\tau$, and the cyclical average Nusselt number $\overline{Nu}_c$ are calculated by the following equations, respectively.

$$Nu_X = -\frac{\partial \theta}{\partial Y} \tag{7}$$

$$\overline{Nu}_X = \frac{1}{w_0} \int_{\overline{BC}} Nu_X \mathrm{d}X \tag{8}$$

$$\overline{Nu}_c = \frac{1}{\tau_p} \int_{\tau_p} \overline{Nu}_X \mathrm{d}\tau \tag{9}$$

where $\tau_p$ is a cyclical time.

For satisfying the boundary conditions at the outlet of the channel, the length from the horizontal channel to the outlet of the right channel is about 70 times the width by numerical tests. In addition, an implicit scheme is implemented to deal with the time differential terms of the governing equations. The time step $\Delta\tau = \frac{1}{60 F_c}$ is chosen for all cases, i.e. totally 60 time steps are required to achieve one periodic cycle.

The dimensionless stream function $\Psi$ is defined as

$$U = \frac{\partial \Psi}{\partial Y}, \quad V = -\frac{\partial \Psi}{\partial X}. \tag{10}$$

In order to show the variations of the flow field more clearly, the streamlines in the vicinity of the horizontal channel are indicated exclusively. Besides, the sign '▲' in the following figures indicates the moving direction of the horizontal channel.

In Fig. 2, the variations of streamlines in one period are indicated for a situation of $Re = 200$, $Gr/Re^2 = 10$, $F_c = 0.2$ and $L_c = 0.5$. Shown in Fig. 2(a), the reciprocating channel completes an upward movement and stops at the highest position. Since the directions of the buoyancy force and inlet cooling fluids are opposite, the cooling fluid streams are suppressed by ascending heat fluids and flow along the right side of the left vertical channel tightly in order to turn to the right and flow into the horizontal channel easily. The impingement region caused by the cooling fluid streams is then deviated slightly from the vertical position. Simultaneously part of heat fluids caused by the buoyancy force flow upwards along the left side of the left vertical channel that leads circulation zones to be observed in the left corner of the heat surface. An opposite flow is apparently indicated in the left vertical channel.

Later on, the cooling fluid streams rush into the horizontal channel and flow along its heated bottom surface; meanwhile, the densities of the cooling fluids neighboring to the heat surface become light. As a result, the cooling fluids intend to depart from the heat surface and separate at about $X = 4.0$. The cooling fluid streams departing from the heat surface tend to move in right and upward direction. A large circulation zone induced by the cooling fluids flow is observed in the space below the cooling fluid streams and near the lower right corner. In the right vertical channel, the directions of the buoyancy force and the cooling fluid streams are consistent, and the cooling fluid streams easily flow out of the channel. An aiding flow is found in the right vertical channel.

In Fig. 2(b), the reciprocating channel moves downwards and has the largest magnitude of downward velocity at that instant. The influence of the buoyancy force is weak. The impingement region is no longer deviated, and the impingement position occurs at $X \approx 0.8$. Due to the influences of the downward movement of reciprocating channel and the inlet cooling fluids, the directions of the cooling fluids in the lower and upper regions of the horizontal channel are rightward and upwards respectively. Near the positions of $X = 3.0$ and 4.5, two circulation zones are separately formed in the central region of the horizontal channel. Afterwards the cooling fluids flow into the right vertical channel.

Shown in Fig. 2(c), the reciprocating channel ends downward movement motion and stops at the lowest position. The buoyancy force changes into a larger magnitude relative to Fig. 2(b). Due to the influence of the downward motion caused by the reciprocating channel, the inlet cooling fluids impinge straightly on the heat surface, and the directions of the cooling fluids in the horizontal channel are changed from approximately vertical (Fig. 2(b)) to horizontal orientations. A reattachment position is found at $X \approx 5.0$.

In Fig. 2(d), the reciprocating channel has the largest upward velocity which makes the buoyancy force in the reciprocating channel to be strong. Consequently, relative to the former ones, the impingement phenomenon weakens remarkably and the cooling fluids almost could not flow tightly along the bottom surface of the horizontal channel. Naturally the reattachment points are hard to be found out. The dual effects of the impulse of cooling fluids and buoyancy force in the right vertical channel cause the cooling fluids to flow straightly in the right vertical channel.

In Fig. 3, the comparisons of local Nusselt numbers of stationary and different periodical states in a cycle are shown for $Re = 200$, $Gr/Re^2 = 10$, $L_c = 0.5$, $F_c = 0.2$ situation. Because of the occurrence of impingement at the inlet region of the heat surface, the largest magnitude of local Nusselt number is then obtained near the inlet region at any stage. According to the reasons mentioned before, the impingement of the cooling fluids on the heat surface at $1/4\tau_p$ and $2/4\tau_p$ stages are stronger than those at $3/4\tau_p$ and $4/4\tau_p$ stages, and then the local Nusselt numbers at $1/4\tau_p$ and $2/4\tau_p$ stages are larger than those of $3/4\tau_p$ and $4/4\tau_p$ stages. Also at the stages of $1/4\tau_p$ and $2/4\tau_p$, the reattachment points exist remarkably which result in convex distributions of local Nusselt numbers near $X = 4.0$ and 5.0, respectively. In most right regions of the heat surface, the directions of the cooling fluid flows and buoyancy force are consistent; the larger local Nusselt numbers could be obtained doubtlessly. However at the stationary state, the fluids in the channel are not disturbed by the reciprocating motion, and the fluids in most right region of the horizontal channel are suppressed by the cooling fluid streams which form a main flow field to lead the cooling fluids to flow out of the channel. Then the local Nusselt numbers near the most right region of the heat surface at the stationary state are smaller than those under the reciprocating situation.

Tabulated in Table 1, the cyclical average Nusselt number $\overline{Nu}_c$ of the situation of $Re = 200$, $Gr/Re^2 = 10$, $F_c = 0.2$ and $L_c = 0.5$ is slightly smaller than that of the situation of $Re = 200$, $Gr/Re^2 = 10$, $F_c = L_c = 0$. The cyclical average Nusselt number $\overline{Nu}_c$ of the situation of $Re = 300$, $Gr/Re^2 = 10$, $F_c = 0.2$ and $L_c = 0.5$ tabulated in Table 1 is larger than that in the corresponding stationary state. Those phenomena imply

**Table 1**
Computed parameters combinations.

| $Re$ | $\frac{Gr}{Re^2}$ | $L_c$ | $F_c$ | $V_m$ | $\overline{Nu}_X$ | $\overline{Nu}_c$ | $\frac{\overline{Nu}_{c,(n)}}{\overline{Nu}_{X,(n)}}$ |
|---|---|---|---|---|---|---|---|
| 200 | 1 | 0 | 0 | 0 | $4.607_{(0)}$ | – | – |
| 200 | 10 | 0 | 0 | 0 | $7.747_{(1)}$ | – | – |
| 300 | 10 | 0 | 0 | 0 | $9.881_{(2)}$ | – | – |
| 200 | 10 | 0.2 | 0.5 | 0.628 | – | $7.674_{(1)}$ | $0.991\left(\frac{\overline{Nu}_{c,(1)}}{\overline{Nu}_{X,(1)}}\right)$ |
| 300 | 10 | 0.2 | 0.5 | 0.628 | – | $10.010_{(2)}$ | $1.013\left(\frac{\overline{Nu}_{c,(2)}}{\overline{Nu}_{X,(2)}}\right)$ |

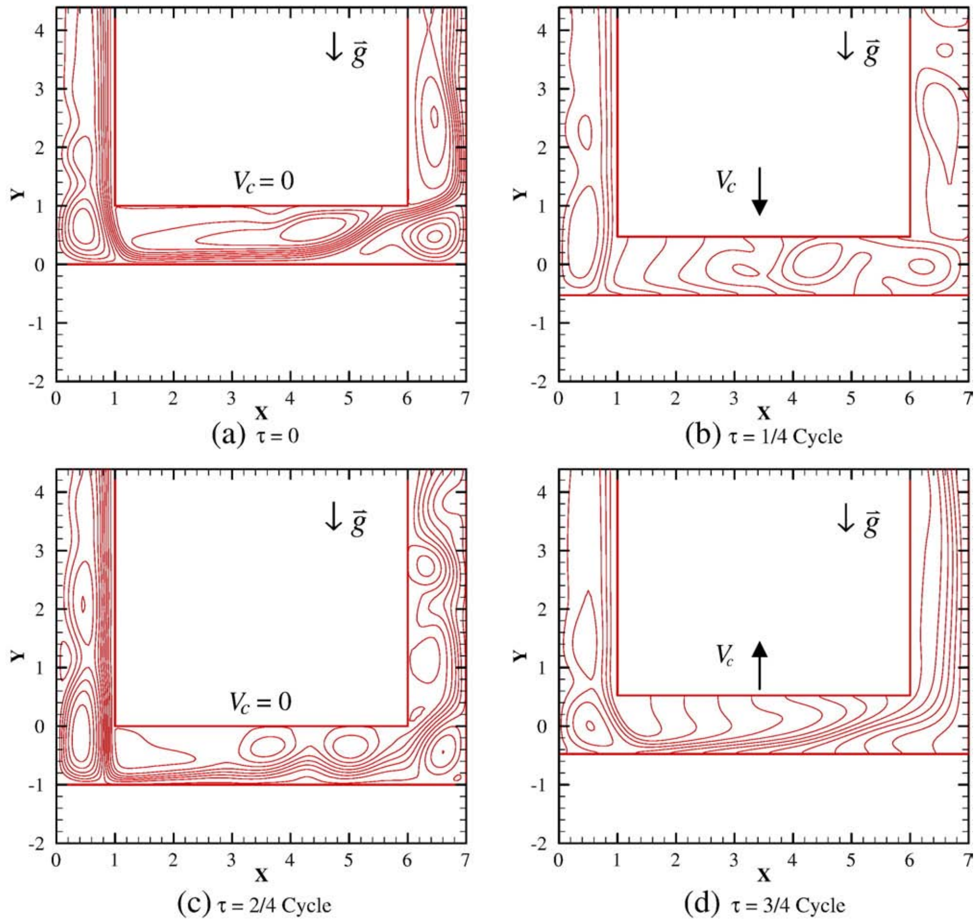


**Fig. 2.** A history of development of distributions of streamlines of one cycle for $Re = 200$, $Gr/Re^2 = 10$, $F_c = 0.2$, and $L_c = 0.5$ situation.

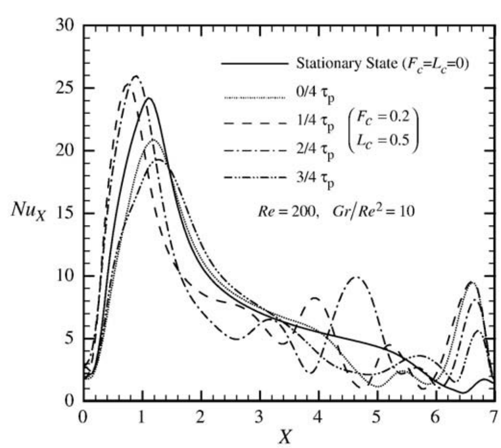


**Fig. 3.** The distributions of local Nusselt numbers of one cycle of $Re = 200$, $Gr/Re^2 = 10$, $F_c = 0.2$, and $L_c = 0.5$ and stationary state.

the enhancement of heat transfer to be affected deeply by the relationship between the buoyancy force and the impulse of cooling fluids.

## 4. Conclusions

Heat transfer phenomena of a mixed convection in a reciprocating channel are investigated numerically and the interesting results are obtained. Some conclusions could be summarized as follows.

(1) Opposite and aiding flows can be observed in the left and right vertical channels, respectively.
(2) Contributions of a reciprocating motion to heat transfer rates are strongly influenced by the relationship between the buoyancy force and impulse of cooling fluids.


## Acknowledgement

The support of this study by the National Science Council of Taiwan, ROC, under contract NSC95-2212-E-009-002 is gratefully acknowledged.


## References


[1] S.W. Chang, L.M. Su, Heat transfer in a reciprocating duct fitted with transverse ribs, Experimental Heat Transfer 12 (1999) 95–115.
[2] W.S. Fu, S.H. Lian, Y.H. Liao, An investigation of heat transfer of a reciprocating piston, International Journal of Heat and Mass Transfer 49 (2006) 4360–4371.